Quasi-Resonant DC-Link Control of Three-Level Active Power Filter

Io-Keong Lok and Man-Chung Wong
Department of Electrical and Electronics Engineering, University of Macau
iokeong.lok@ieee.org

Abstract-**This paper presents a three-level three-phase four-wire active power filter with a quasi-resonant dc-link (QRDCL) soft-switching auxiliary circuit. The three-level quasi-resonant dc-link circuit is constructed by two symmetrical two-level quasi-resonant dc-link snubbers and each snubber can be operated independently. Its operating principle is presented in this paper. Additionally, a direct pulse width modulation (PWM) is employed which can simplify the calculation and can be easily implemented in a digital signal processor (DSP). Simulation of the three-level soft-switched active power filter is provided. Switching losses between the hard switching and soft switching of active power filter is also illustrated.**

I. INTRODUCTION

Contrast to conventional two-level inverters, three-level inverters not only relax the voltage stress and switching frequency on the switching devices, but also provide more available voltage vectors, which can improve the flexibility and the performance of the inverters in the area of power quality compensation [1], [2]. Applying soft switching techniques into three-level inverters can reduce switching losses of inverters in order to increase the efficiency and prolong the lifetime of the devices [3].

In this paper, a quasi-resonant dc-link circuit in three-level inverters for three-phase four-wire power quality compensation is presented. In contrast to some soft switching techniques [4], [5], in which the duration of zero voltage is too expeditious that the zero voltage switching of a device cannot be fully achieved under the existence of tail current of IGBTs [6]. The duration of zero voltage can be extended by using the QRDCL circuit in this paper. The three-level QRDCL circuit is constructed by two symmetrical two-level QRDCL snubbers. By operating two symmetric QRDCL circuits, the dc link voltage of the inverter could decrease to zero and provides zero voltage switching conditions for the inverter's main switches. In addition, the auxiliary switches can also be switched under soft switching conditions. However, the QRDCL operation interacts between phases in a three-phase system, and due to the extended duration of zero voltage, the effective pulse width of each phase is shortened and hence the performance of the compensator is affected. Therefore, a correction on pulse width modulation (PWM) is also presented, which can minimize the deterioration of the performance caused by the soft switching operation. Simulation results have been given to show that the switching losses have been reduced significantly after applying the soft switching technique. And the improvement of using corrected pulse width has also been proved in the simulation. The three-phase four-wire compensation system is shown in Fig. 1, in which harmonics unbalance and reactive power are injected by non-linear load.

II. QUASI-RESONANT DC-LINK INVERTER

In order to extend the duration of zero voltage [7], the control strategy of QRDCL for three-level inverter is proposed, in which the duration of zero voltage can be controlled by managing the trigger of the auxiliary switches S_a, S_b, and S_c

Fig. 2 shows the upper QRDCL circuit which is constructed by three auxiliary switches S_a, S_b and S_c, a resonant inductor L_r and a resonant capacitor C_r. According to the operation waveforms, the QRDCL circuit can be divided into five operational modes.

Mode 0: The inverter is in normal condition, in which no commutation happened. S_c is conducted and let the load current going through.

Mode 1: Switch S_b is conducted and current starts going through the inductor rapidly to an initial value I_i, which can be obtained by (1).

$$I_i = \frac{V_{DC}}{4 \cdot L_r} \cdot T_1 \cdot \tag{1}$$

Mode 2: Resonance occurs between capacitor C_r and inductor L_r when Sc is turned off. Voltage V_{cr} decreases to zero rapidly with initial current I_i. The corresponding capacitor voltage and the duration of T_2 can be calculated by (2) and (3) respectively.

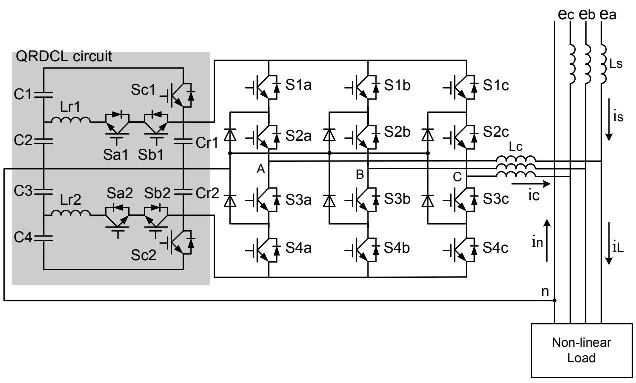

Fig. 1. Three-level power quality compensator with QRDCL circuit.

$$V_{cr}=\frac{V_{DC}}{2}\cdot\cos(\omega_r t)-Z_r(I_i-I_o)\sin(\omega_r t), \quad (2)$$

$$T_2=\frac{1}{\omega_r}\tan^{-1}\left(\frac{V_{DC}}{2\cdot(I_i-I_o)}\right), \quad (3)$$

where $\omega_r=\frac{1}{\sqrt{L_r C_r}}$, and $Z_r=\sqrt{\frac{L_r}{C_r}}$.

Mode 3: Zero voltage switching can be achieved for the main switches of the inverter. Auxiliary switch S_b turns off under zero current condition. Moreover, the voltage can be kept zero temporary until auxiliary switch S_a is turned on.

Mode 4: S_a is conducted in order to recharge the capacitor voltage. The capacitor voltage increases while the inductor current is larger then the load current. The duration of T_4 can be calculated by (4).

$$T_4=\frac{2\cdot L_r I_o}{V_{DC}}+\pi\sqrt{L_r C_r}, \quad (4)$$

Mode 5: The capacitor voltage returns to its original level and auxiliary switch S_c turns on under zero voltage condition. The inductor current decreases to zero and S_a is turned off under zero current switching.

Notification signal of zero voltage condition can be sent to the PWM control when entering Mode 3. Switching state of the two-level inverter can be changed and the switching losses of the power devices of the inverter can be greatly reduced.

III. Control of Active Power Filter

The control system of a quasi-resonant dc-link three-level active power filter can be divided into three parts, which are the calculation of reference currents for compensation, the control of pulse width modulation and the control of the quasi-resonant dc-link. Their operations will be discussed in detail in the following paragraphs.

A. *Instantaneous reactive power*

Well-known instantaneous reactive power theory had been widely used in active power applications for calculating reference currents, and the instantaneous reactive power control in three-phase four-wire is employed in this paper [8]. According to the instantaneous reactive power theory, the system voltage and the load current are transformed from a-b-c coordinates into 0-α-β coordinates by using the transformations (5) and (6):

$$\begin{bmatrix} e_0 \\ e_\alpha \\ e_\beta \end{bmatrix}=\sqrt{\frac{2}{3}}\begin{bmatrix} 1/\sqrt{2} & 1/\sqrt{2} & 1/\sqrt{2} \\ 1 & -1/2 & -1/\sqrt{2} \\ 0 & \sqrt{3}/2 & -\sqrt{3}/2 \end{bmatrix}\cdot\begin{bmatrix} e_a \\ e_b \\ e_c \end{bmatrix}, \quad (5)$$

$$\begin{bmatrix} i_{L0} \\ i_{L\alpha} \\ i_{L\beta} \end{bmatrix}=\sqrt{\frac{2}{3}}\begin{bmatrix} 1/\sqrt{2} & 1/\sqrt{2} & 1/\sqrt{2} \\ 1 & -1/2 & -1/\sqrt{2} \\ 0 & \sqrt{3}/2 & -\sqrt{3}/2 \end{bmatrix}\cdot\begin{bmatrix} i_{La} \\ i_{Lb} \\ i_{Lc} \end{bmatrix}, \quad (6)$$

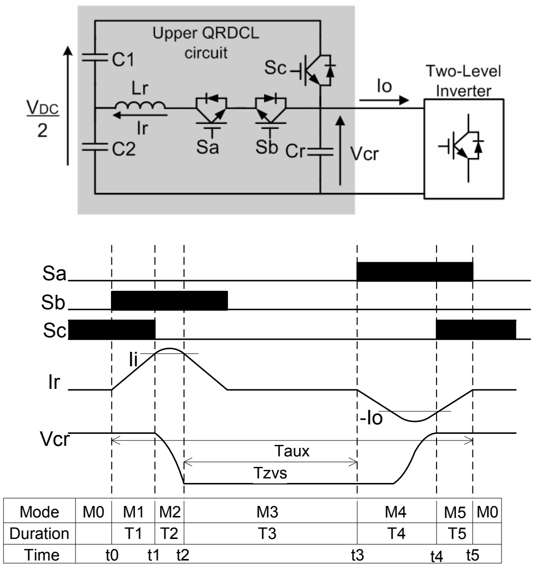

Fig. 2. The QRDCL configuration and its operation waveforms.

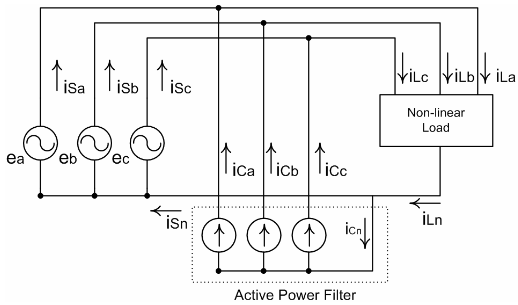

Fig. 3. Three-phase four-wire active power filter.

where e_a, e_b and e_c are the system voltages, and i_{La}, i_{Lb} and i_{Lc} are the load currents as shown in Fig. 3.

Therefore the instantaneous real power p_{L0} and $p_{L\alpha\beta}$, and an instantaneous imaginary power $q_{L\alpha\beta}$ in the three-phase four-wire system can be obtained as follow:

$$\begin{bmatrix} p_{L0} \\ p_{L\alpha\beta} \\ q_{L\alpha\beta} \end{bmatrix}=\begin{bmatrix} e_0 & 0 & 0 \\ 0 & e_\alpha & e_\beta \\ 0 & -e_\beta & e_\alpha \end{bmatrix}\cdot\begin{bmatrix} i_{L0} \\ i_{L\alpha} \\ i_{L\beta} \end{bmatrix}. \quad (7)$$

The compensating currents on 0-α-β coordinates are calculated in terms of the real power and the imaginary power of the active power filter as (8).

$$\begin{bmatrix} i_{C0} \\ i_{C\alpha} \\ i_{C\beta} \end{bmatrix}=\frac{1}{e_0 e_{\alpha\beta}^2}\begin{bmatrix} e_{\alpha\beta}^2 & 0 & 0 \\ 0 & e_0 e_\alpha & -e_0 e_\beta \\ 0 & e_0 e_\beta & e_0 e_\alpha \end{bmatrix}\cdot\begin{bmatrix} p_{C0} \\ p_{C\alpha\beta} \\ q_{C\alpha\beta} \end{bmatrix}, \quad (8)$$

where

$$e_{\alpha\beta}^2=e_\alpha^2+e_\beta^2$$

By establishing the following relations:

$$p_{C0} = p_{L0}$$
$$p_{C\alpha\beta} = \tilde{p}_{L\alpha\beta}, \quad (9)$$
$$q_{C\alpha\beta} = q_{L\alpha\beta}$$

in which $\tilde{p}_{L\alpha\beta}$ is the ac component of $p_{L\alpha\beta}$.

The power flow of active power filter contains the active power of harmonic currents and also the reactive power of the entire system, therefore both harmonics and reactive power in the system can be fully compensated by the active power filter. After substituting the above relations into equation, the compensating currents in 0-α-β coordinates are expressed as:

$$i_{C0} = \frac{1}{e_0} p_{L0} = \frac{1}{e_0} \cdot e_0 i_{L0} = i_{L0} \cdot \quad (10)$$

$$i_{C\alpha} = \frac{1}{e_{\alpha\beta}^2}\left(e_\alpha \cdot \tilde{p}_{L\alpha\beta} - e_\beta \cdot q_{L\alpha\beta}\right) \cdot \quad (11)$$

$$i_{C\beta} = \frac{1}{e_{\alpha\beta}^2}\left(e_\beta \cdot \tilde{p}_{L\alpha\beta} + e_\alpha \cdot q_{L\beta}\right) \cdot \quad (12)$$

The compensating currents on a-b-c coordinates can be obtained by using the inversed transformation matrix of (6). These reference currents will be transferred into reference voltages V_{ref}, according to the output impedance of the active power filter.

B. Direct pulse width modulation

Many pulse width modulations have been proposed for multilevel converters in three-phase four-wire system, but a three-dimensional (3-D) generalized direct PWM, which was proposed in 2005 [9], is employed in the paper. Among the other PWM algorithms, the direct PWM has the advantage which greatly simplifies the calculation process so that it is much easier to implement in digital signal controllers. The computational cost of the direct PWM is much lower because the case determination chart and switching time table are not needed. Moreover, the modulation outputs are proved that they are the same as those of 3-D space vector modulation.

An equivalent model for N-level inverter is shown in Fig 4, in which the phase output voltage can be expressed as (13).

$$V_j = m_j \cdot E \qquad j = a,b,c \text{ and } 0 \le m_j \le N-1, \quad (13)$$

where m_j denotes the switching state of the corresponding phase and E denotes the dc voltage of one level. In the generalized direct PWM, the reference voltage vector is normalized and decomposed into two components: the offset voltage vector and the two-level voltage vector.

$$\vec{v}_{ref} = \frac{\vec{V}_{ref}}{E}, \quad (14)$$

$$\vec{v}_{ref} = \vec{v}_{offset} + \vec{v}_{twol}, \quad (15)$$

where

$$\vec{v}_{offset} = INT(\vec{v}_{ref}).$$

INT() removes the fractional part of the normalized voltage vector, and the two-level vector will be used to directly determine the final pulse width. If ($v_{offset,a}$, $v_{offset,b}$, $v_{offset,c}$) equals (m_a, m_b, m_c), the reference voltage vector will be located inside the two-level space vector allocation which

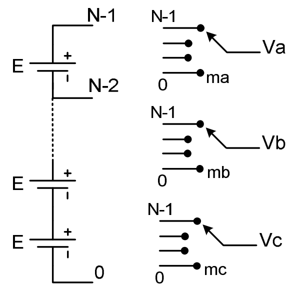

Fig. 4. Equivalent model of N level inverter.

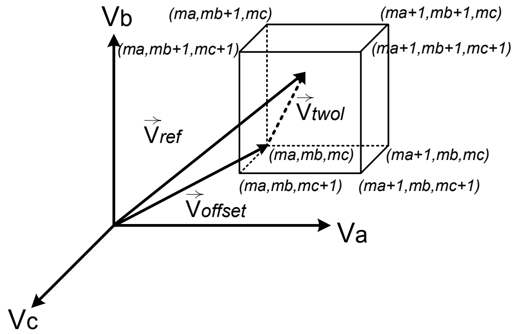

Fig. 5. Decomposition of reference voltage vector.

formed by (m_a, m_b, m_c), (m_a+*1*, m_b, m_c), (m_a, m_b+*1*, m_c), (m_a, m_b, m_c+*1*), (m_a+*1*, m_b+*1*, m_c), (m_a+*1*, m_b, m_c+*1*), (m_a, m_b+*1*, m_c+*1*), (m_a+*1*, m_b+*1*, m_c+*1*) as illustrated in Fig. 5. Based on the volt-time product approximation just as in conventional space vector modulation (SVM), the pulse width of each phase can be calculated, and the reference voltage vector is synthesized in phases A, B and C independently, as (16).

$$v_{ref,j} \cdot T_S = v_{offset,j} \cdot t_{off,j} + \left(v_{offset,j} + 1\right) \cdot t_{on,j} \qquad j = a,b,c, \quad (16)$$

where T_S is the sampling period, $t_{off,j}$ is the dwell time of the output state m_j, $t_{on,j}$ is the dwell time the output state m_j+1, and $t_{off,j}$+ $t_{on,j}$ =T_S. Therefore, the pulse width of each phase can be calculated from the two-level voltage vector as (17) and (18) by subtracting $v_{offset,j} \cdot T_S$ from both side of (16).

$$t_{on,j} = v_{twol,j} \cdot T_S \qquad j = a,b,c, \quad (17)$$

$$t_{off,j} = \left(1 - \left|v_{twol,j}\right|\right) \cdot T_S = T_S - t_{on,j} \qquad j = a,b,c. \quad (18)$$

C. Control of QRDCL

If no commutation is needed, the QRDCL control will be running in steady mode, in which the auxiliary switch S_c is conducted and, S_a and S_b are not conducted. The control of QRDCL is activated when a new pattern of PWM is detected. The PWM signals are held by a latch device and wait for the confirmation of zero voltage condition. The switching signals of the auxiliary switches are sent to the soft switching circuit to perform a dc-link resonance. As the zero dc voltage is detected, the latch is enabled and outputs the latest pattern of PWM signals. As the detail operation of QRDCL is discussed in Section II, the control flow of the QRDCL circuit is illustrated as Fig. 6. Additionally, Fig. 7 shows the

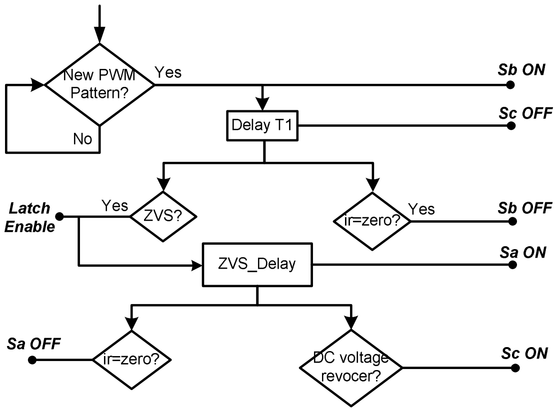

Fig. 6. Control of QRDCL.

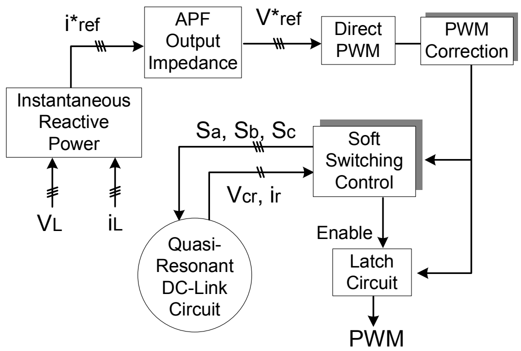

Fig. 7. Control of active power filter with QRDCL.

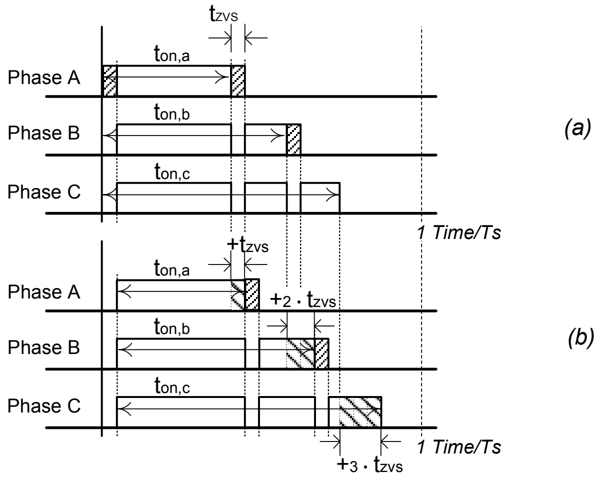

Fig. 8. (a) The effect of soft switching on effective pulse width and, (b) the correction of adding extra pulse width

overall control diagram of three-level active power filter with the control of QRDCL.

IV. Correction of Pulse Width Modulation

According to the operations of QRDCL in Section II, the duration of zero voltage is being extended. And the extended zero voltage condition could help the power devices to have a more complete zero voltage switching. However this could result in an instant zero voltage output in all three phases, as illustrated in Fig. 8(a). The zero voltage effect causes a shortage on the effective pulse width on all three phases. The longest pulse width will suffer the most serious effect of zero output voltage. The final output voltage of each phase will be smaller than the desired value, and this affects the compensation performance of the inverter while the output vectors are deviated from its reference vector. Therefore, additional time is added into the pulse width in order to extend its effective duration as illustrated in Fig. 8(b). According to the length of the pulse width, each of them will be extended 1, 2 or 3 times of the duration of zero voltage, T_{ZVS}. The corrected final pulse width of each phase can be expressed as (19).

$$t^{*}_{on,j} = t_{on,j} + n \cdot t_{ZVS} \qquad j = a,b,c \;\; and \quad n = 1,2 \; or \; 3 . \tag{19}$$

V. Simulation Results

The three-level active power filter with QRDCL in three-phase four-wire system as illustrated in Fig. 1 is simulated in PSCAD/EMTD, in which the harmonics and reactive power were injected by the non-linear load. In order to test the performance of three-level active power filter, a serious current distortion with total harmonic distortion (THD) up to 40% is generated and accompany with a power factor of 0.9. After the compensation, a target of THD lower than 10% with power factor 0.99 had been achieved.

The system parameters of three-level active power filter with QRDCL are listed in Table 1. Fig. 9 shows the source currents before the compensation. Fig. 10 and Fig. 11 show the source current after the compensation with and without applying soft switching technique. The simulations show that both hard switching and soft switching could compensate the nonlinear current very well and could relax the current flowing through the neutral line. Fig. 12 also shows the switching losses of the thee-level QRDCL active power filter before and after the operation of QRDCL circuit. The figure shows that the switching losses had been reduce significantly when the soft switching is applied, and the switching stresses of the power devices are released as shown in the switching transients of Fig. 13.

TABLE I
System Parameters in The Simulation

System Parameters	Symbols	Value
Source voltage(rms)	Es	110 V
Source frequency	f	50 Hz
Compensating inductance	Lc	10 mH
dc-Link voltage	Vdc	800 V
Switching frequency	fs	5000 Hz
Resonant inductance	Lr	5 µH
Resonant capacitance	Cr	0.1 µF

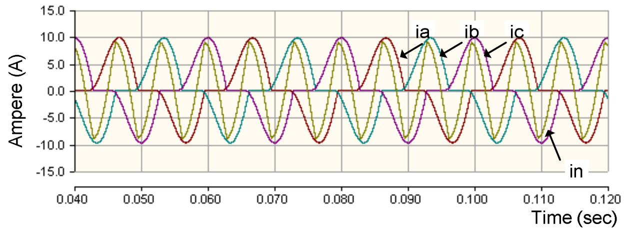

Fig. 9. Source currents before the compensation.

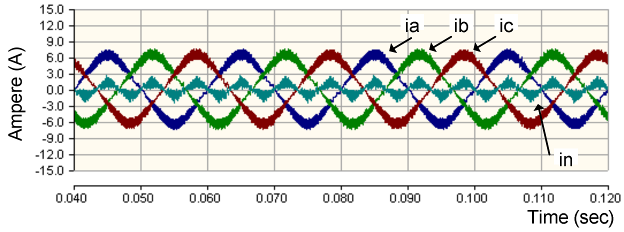

Fig. 10. Source currents after the compensation with QRDCL.

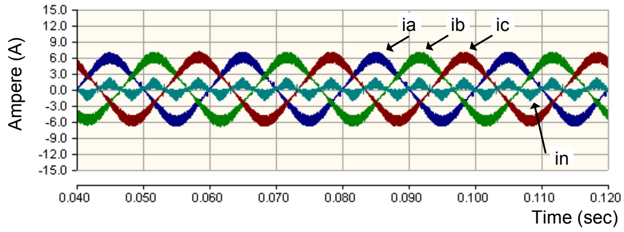

Fig. 11. Source currents after the compensation without QRDCL.

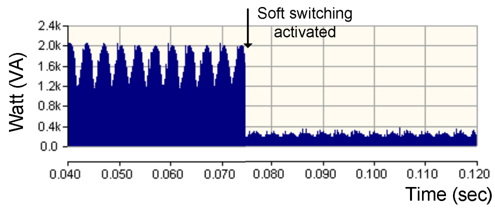

Fig. 12. Switching losses before and after activating the QRDCL.

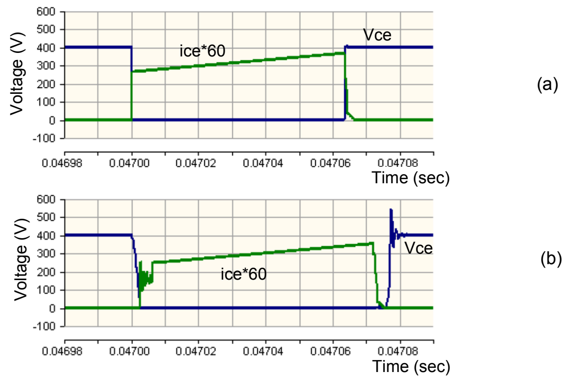

Fig. 13. Switching transients of (a) hard switching and (b) soft switching.

Table II shows the compensation results of hard switching, soft switching without the correction of PWM and soft switching with the correction of PWM. It shows that the compensating performance is slightly decreased with the deteriorated PWM. However, the compensating performance has been improved after applying the correction of PWM.

TABLE II
SIMULATION RESULTS OF THREE-LEVEL QRDCL ACTIVE POWER FILTER

	Before compensation	After compensation		
		Hard switching	Soft switching w/o PWM correction	Soft switching w. PWM correction
THD	39.4%	5.1%	6.5%	5.6%
Neutral current (rms)	5.9A	0.71A	0.89A	0.81A
Power Factor	0.9	0.99	0.99	0.99
Switching losses (average)	-	10W	5.3W	5.3W

VI. CONCLUSION

A quasi-resonant dc-link control of three-level active power filter is proposed and simulated. The results show that the proposed active power filter can also compensate the nonlinear current and reactive power very well. With the extended zero voltage duration, switching losses has been significantly reduced. And by adding a PWM correction control, the performance deterioration of using soft switching techniques can be eliminated.

ACKNOWLEDGMENT

This work is supported by The Science and Technology Development Fund (FDCT) of Macau S.A.R., and the Research Committee of University of Macau.

REFERENCES

[1] Jose Rodrigues, Jim-Sheng Lai and Fang Zheng Peng, "Multilevel inverters: a survey of topologies, controls and applications", IEEE Trans. Ind. Electronics, vol. 49, pp.724–738, August 2002.
[2] Ning-Yi Dai, Man-Chung Wong and Ying-Duo Han, "Application of a three-level npc inverter as a three-phase four-wire power quality compensator by generalized 3DSVM", IEEE Trans. on Power Electronics, vol. 21, pp.440–449, March 2006.
[3] Maria D. Bella, Tzong-Shiann Wu, Aristide Tchamdjou, Javad Mahdavi and M. Ehsani, "A review of soft-switched dc-ac converters", IEEE Trans. Ind. Applications, vol. 34, pp.847–860, July 1998.
[4] Jie Chang and Jun Hu, "Modular design of soft-switching circuits for two-level and three-level inverters", IEEE Trans. on Power Electronics, vol. 21, pp.131–139, January 2006.
[5] M. Yamamoto, H. Iwamoto, E. Hiraki, T. Horiuchi, Y. Sugawara and M. Nakaoka, "3-level 3-phase voltage-fed soft-switching inverter with new space voltage vector modulation scheme and its feasible evaluations", Power Electronics and Variable Speed Drives, no.475, pp.541–547, September 2000.
[6] Trivedi M., Pendharkar, S. and Shenai, K., "Switching characteristics of MCT's and IGBT's in power converters", IEEE Trans. Electron Devices, vol. 43, pp.1994–2003, November 1996.
[7] Ming-hui Zhan, Man-Chung Wong and Ying-duo Han, "Quasi-resonant dc link control of 3-dimensional hysteresis current pwm technique in 3-phase 4-wired power quality compensator", IEEE Transmission and Distribution Conference, pp.1–6, 2005
[8] Akagi, H, Ogasawara, S, Hyosung Kim, "The theory of instantaneous power in three-phase four-wire systems: a comprehensive approach", Industry Applications Conference, vol. 1, pp. 431–439, October 1999.
[9] Ning-Yi Dai, Man-Chung Wong, Yuan-Hua Chen and Ying-Duo Han, "A 3-D generalized direct pwm algorithm for multilevel converters", IEEE Power Electronics Letters, vol. 3, pp.85–88, September 2005.